

## **Ferredoxin:NADP(H) Oxidoreductase Abundance and Location Influences Redox Poise and Stress Tolerance.**

Kozuleva, M; Goss, T; Twachtmann, M; Rudi, K; Trapka, J; Selinski, J; Ivanov, B; Garapati, P; Steinhoff, HJ; Hase, T; Scheibe, R; Klare, JP; Hanke, GT

Copyright © 2016 by the American Society of Plant Biologists

This is a pre-copyedited, author-produced PDF of an article accepted for publication in Plant Physiology following peer review. The version of record is available

<http://www.plantphysiol.org/content/172/3/1480.short>

For additional information about this publication click this link.

<http://qmro.qmul.ac.uk/xmlui/handle/123456789/17677>

Information about this research object was correct at the time of download; we occasionally make corrections to records, please therefore check the published record when citing. For more information contact [scholarlycommunications@qmul.ac.uk](mailto:scholarlycommunications@qmul.ac.uk)

**Short Title:** FNR abundance and location in the stress response

**Corresponding Author:**

Guy Hanke  
Queen Mary University of London  
Mile End Road, E1 NS4, UK  
Tel: 020 7882 6483

**Title:** Ferredoxin:NADP(H) oxidoreductase abundance and location influences redox poise and stress tolerance

**Kozuleva, M.<sup>1</sup>, Goss, T.<sup>2</sup>, Twachtmann, M.<sup>2</sup>, Rudi, K.<sup>3</sup>, Trapka, J.<sup>2</sup>, Selinski, J.<sup>2</sup>, Ivanov, B.<sup>1</sup>, Garapati. P.<sup>2</sup>, Steinhoff, H.-J.<sup>3</sup>, Hase, T.<sup>4</sup>, Scheibe, R.<sup>2</sup>, Klare, J.P.<sup>3</sup>, Hanke, G.T.<sup>2,5</sup>**

<sup>1</sup>Institute of Basic Biological Problems, Russian Academy of Sciences, Puschino, 142290 Russia

<sup>2</sup>Department of Plant Physiology, Osnabrück University, Osnabrück 49076, Germany

<sup>3</sup>Department of Biophysics, Osnabrück University, Osnabrück 49076, Germany

<sup>4</sup>Institute for Protein Research, Osaka University, 3-2 Yamadaoka, Suita-shi, Osaka 565-0871, Japan

<sup>5</sup>School of Biochemistry and Chemistry, Queen Mary University of London, E1 4NS, England

**One Sentence summary:** The abundance and location of ferredoxin:NADP(H) oxidoreductase in the chloroplast influences free radical production, chloroplast redox poise and plant stress perception

**Author Contributions:**

G.T.H., M.K., J.P.K., T.H. and R.S. conceived the original research plan; G.T.H, T.H., R.S. H.-J. S. and J.K. supervised the experiments; G.T.H., T.G., M.K., J.P.K., R.K. performed most of the experiments; M.T., P.G. and J.S performed some of the experiments; M.K, G.T.H and J.P.K analyzed most of the data; G.T.H. wrote the article with contributions from all the authors.

**Funding Information:**

The authors gratefully acknowledge financial support from the Deutsche Forschungsgemeinschaft through funding of Project 2 in the Collaborative Research Center (SFB) 944 at the University of Osnabrück. M.K. was supported by grant HA 5921/2-1 for the initiation of international collaboration.

**Corresponding author e-mail:** g.hanke@qmul.ac.uk

## Abstract

In linear photosynthetic electron transport, ferredoxin:NADP(H) oxidoreductase (FNR) transfers electrons from ferredoxin (Fd) to NADP<sup>+</sup>. Both NADPH and reduced Fd (Fd<sup>red</sup>), are required for reductive assimilation and light/dark activation/deactivation of enzymes. FNR is therefore a hub, connecting photosynthetic electron transport to chloroplast redox metabolism. A correlation between FNR content and tolerance to oxidative stress is well established, although the precise mechanism remains unclear. We investigated the impact of altered FNR content and localization on electron transport and superoxide radical evolution in isolated thylakoids, and probed resulting changes in redox homeostasis, expression of oxidative stress markers and tolerance to high light *in planta*. Our data indicate that the ratio of Fd<sup>red</sup> to FNR is critical, with either too much or too little FNR potentially leading to increased superoxide production, and perception of oxidative stress at the level of gene transcription. In FNR overexpressing plants, which show more reduced NADP(H) and glutathione pools, improved tolerance to high-light stress indicates that disturbance of chloroplast redox poise and increased free radical generation may help “prime” the plant and induce protective mechanisms. In *fnr1* knock-outs, the NADP(H) and glutathione pools are more oxidized relative to the wt, and the photoprotective effect is absent despite perception of oxidative stress at the level of gene transcription.

## INTRODUCTION

In photosynthetic electron transport (PET), electrons are accepted at photosystem I (PSI) by ferredoxin (Fd), before being transferred to the flavo-enzyme ferredoxin:NADP(H) oxidoreductase (FNR). PSI, Fd and FNR are reported to be present at a 1:5:3 ratio in spinach chloroplasts (Bohme, 1978). Very high control coefficients of FNR for photosynthesis of 0.94 (at saturating light) and 0.7 (at limiting light) were calculated from a study on antisense tobacco plants with variable FNR concentrations (Hajirezaei et al., 2002). In higher plants, FNR enzymes have a dynamic relationship with the membrane, being recruited to various membrane complexes (Andersen et al., 1992; Jose Quiles and Cuello, 1998; Zhang et al., 2001) including the two dedicated FNR-tethering proteins Tic62 (Benz et al., 2009) and TROL (Juric et al., 2009). Interaction of FNR with Tic62 and TROL is dependent on the LiR1 protein (Yang et al., 2016) and is regulated by pH (Alte et al., 2010; Lintala et al., 2014). The catalytic cycle of FNR is well described (Batie and Kamin, 1981, 1984, 1986; Carrillo and Ceccarelli, 2003; Cassan et al., 2005), with two reduced Fd ( $Fd^{red}$ ) molecules binding in sequence to reduce the flavin cofactor before reduction of one  $NADP^+$ . There is strong evidence for formation of a ternary complex (Martinez-Julvez et al., 2009).

During light excitation, the PET chain is a rich source of reactive oxygen species (ROS). Superoxide radical ( $O_2^{\cdot-}$ ) produced mainly at photosystem I (PSI) (Allen and Hall, 1974), and singlet oxygen ( $^1O_2$ ) produced at photosystem II (PSII) (Telfer et al., 1994) are the dominant species evolved. Due to the damaging nature of ROS, very efficient scavenging (or antioxidant)- mechanisms exist in chloroplasts to prevent oxidative damage:  $^1O_2$  can be quenched by  $\beta$ -carotene,  $\alpha$ -tocopherol or plastoquinone (Krieger-Liszkay et al., 2008), while in the water-water cycle (Asada, 1999)  $O_2^{\cdot-}$  is rapidly converted to  $H_2O_2$  by superoxide dismutase (SOD) enzymes or plastoquinol (Mubarakshina and Ivanov, 2010).  $H_2O_2$  can be converted to the highly damaging  $OH^{\cdot}$  radical in the Fenton reaction by any of the multiple iron, copper or manganese centers in the thylakoid membrane or free ions (Snyrychova et al., 2006). To prevent this, the chloroplast is rich in proteins that reductively convert  $H_2O_2$  to  $H_2O$ , such as peroxiredoxin, which can be reduced by either thioredoxin (Konig et al., 2002) or the NADPH dependent thioredoxin reductase C (NTRC) (Pulido et al., 2010), and other peroxidase enzymes, which use ascorbate as the electron donor (Mittler et al., 2004; Foyer and Noctor, 2011). Ascorbate can be directly regenerated using photosynthetic electrons via  $Fd^{red}$  (Asada, 1999). Alternatively, dehydroascorbate reductase can reduce ascorbate using reduced glutathione (GSH). In the chloroplast, the oxidized glutathione (GSSG) is re-reduced by the glutathione reductase 2 (GR2) enzyme (Chew et al., 2003) using NADPH. It is now well established that retrograde signaling from the chloroplast controls gene expression and that oxidative species contribute to this signaling pathway (Mittler et al., 2004; Oelze et al., 2008;

Mubarakshina Borisova et al., 2012). A balance therefore exists between rapid removal of damaging oxidative species and maintenance of appropriate concentrations necessary to initiate signaling cascades. A simplified diagram showing the interconnections between FNR, the ( $\text{Fd}^{\text{red}} / \text{Fd} + \text{e}^-$ ) and ( $\text{NADPH} / \text{NADP}^+ + \text{H}^+ + 2\text{e}^-$ ) redox couples and redox homeostasis is shown in Figure 1.

In addition to its classical role in photosynthesis, there is a well-established connection between FNR and oxidative stress. This was first discovered in *Escherichia coli*, where the equivalent (though non-photosynthetic) protein was found to be a diaphorase of the  $\text{O}_2^-$  generator methyl viologen (MV), and was also identified as a member of the stress-responsive *soxRS* regulon (Liochev et al., 1994). Overexpression of FNR in *E. coli* caused an upregulated *soxRS* response, and mutants lacking FNR were found to be more susceptible to MV-mediated oxidative stress, although the *soxRS* response was not affected (Krapp et al., 2002). Furthermore, it was discovered that higher plant FNR was capable of rescuing mutants of the *E. coli* gene (Krapp et al., 1997). It was suggested that FNR could act to balance the NADPH redox poise, thus affecting expression of the *soxRS* regulon. Alternative mechanisms by which FNR could promote tolerance to oxidative stress include potentially transferring electrons from NADPH to scavengers of ROS, acting in the repair of iron centers, or even by functioning as an anti-oxidant itself (Krapp et al., 1997; Krapp et al., 2002; Giro et al., 2006).

An analogous connection to the stress response was discovered for higher plant FNR in work on antisense of tobacco (*Nicotiana tabacum*) FNR, which showed decreased chlorophyll, carotenoids and photosynthetic capacity, and increased lipid peroxidation and membrane leakage upon high-light treatment (Palatnik et al., 2003). Staining of whole leaves for ROS indicated that acceptor limitation at PSI caused an increased reduction state of the electron transport chain and  $^1\text{O}_2$  production. In addition, over-expression of pea (*Pisum sativum*) FNR in tobacco has been shown to afford protection from oxidative stress (Rodriguez et al., 2007). When subjected to MV-mediated oxidative stress the over-expressing plants showed less membrane leakage, chlorophyll loss and damage to PSII than the wt. Mirroring the work on tobacco, it has been reported that single mutants of both *Arabidopsis thaliana* genes, *FNR1* and *FNR2*, show increased membrane leakage when challenged with MV (Lintala et al., 2009). In the same study the authors found an isoform-specific effect, with *fnr2* knock-downs proving more tolerant than wt or *fnr1* knock-outs to high-light stress at low temperatures. In *fnr2* knock-downs, the remaining FNR1 is membrane-bound, while in *fnr1* mutants all remaining FNR2 is soluble. Intriguingly, there is other evidence for a relationship between FNR location within the chloroplast and oxidative stress. In tobacco, MV-derived, PET-dependent oxidative stress causes the solubilization of FNR (Palatnik et al., 1997), and it was recently reported that chloroplasts from *Arabidopsis trol* mutants, which lack one of the

FNR-thylakoid tethering proteins, generate lower amounts of superoxide than wt upon illumination (Vojta et al., 2015).

We previously generated Arabidopsis plants with increased FNR, by over-expressing genes for different maize (*Zea mays*) FNR proteins under control of the native Arabidopsis promoter (Twachtmann et al., 2012). We used ZmFNR3, which is predominantly soluble, and ZmFNR1, which can bind to the thylakoid membrane when expressed in Arabidopsis. This resulted in FNR contents 1.5-2 times that of the wt. These enzymes have nearly identical catalytic properties (Okutani et al., 2005), that are similar to those of the native Arabidopsis FNRs (Hanke et al., 2005), meaning that the major difference between over-expression of ZmFNR1 and ZmFNR3 lies in the chloroplast localization of the introduced enzymes. To better understand the impact of FNR content and location on plant stress tolerance, we have compared NADP<sup>+</sup> and glutathione redox poise, O<sub>2</sub><sup>-</sup> generation and responsive genes, and high-light stress response in plants expressing ZmFNR1 and ZmFNR3 and *fnr1* mutants, which lack membrane bound FNR. Our data provide evidence that the content and location of FNR affect the redox balance of the chloroplast, with knock-on effects on redox signaling and stress tolerance.

## RESULTS

### FNR content correlates with redox poise of the NADP(H) pool

In order to understand how FNR abundance and localization in Arabidopsis affects NADP<sup>+</sup> photoreduction, and to examine the downstream effects of this, we first selected two genotypes with extreme differences in FNR content and location. In Arabidopsis *fnr1* mutants, no FNR remains bound to the thylakoid (Lintala et al., 2007; Hanke et al., 2008), and over-expression of maize *FNR1* (ZmFNR1) in Arabidopsis results in enhanced accumulation of FNR at the thylakoid, specifically at TROL-dependent complexes (Twachtmann et al., 2012). Total FNR activity of the thylakoids from these genotypes confirms this (Figure 2A). While there is no difference in total electron flux by thylakoids from wt, *fnr1*, and ZmFNR1 expressing plants (Figure 2B), the difference in FNR contents translate into decreased NADP<sup>+</sup>-photoreduction capacity of *fnr1* thylakoids, and increased NADP<sup>+</sup>-photoreduction capacity in thylakoids from ZmFNR1 plants (Figure 2C). This is in agreement with work on FNR-over-expressing tobacco, where a 20% stimulation of NADP<sup>+</sup>-photoreduction in isolated thylakoids was measured (Rodriguez et al., 2007), indicating that membrane-bound FNR can photoreduce NADP<sup>+</sup>. In the wt rates of electron flux to NADP<sup>+</sup> (Figure 2C) are about one third to half the capacity for total electron flux from H<sub>2</sub>O (Figure 2B). This suggest that either loosely bound or soluble FNR lost in thylakoid preparation might be required for maximum rates of

electron flow to NADP<sup>+</sup>, or that FNR capacity limits flux to NADP<sup>+</sup>, as suggested by the antisense work in tobacco (Hajirezaei et al., 2002).

We then tested whether the redox poise of NADP(H) (the NADP<sup>+</sup>/NADP(H) ratio) reflects the thylakoid capacity for NADP<sup>+</sup> photoreduction. The redox state of the chloroplast NADP(H) pool is very accurately reflected in the activation state of the NADP-malate dehydrogenase (NADP-MDH) (Scheibe and Stitt, 1988), reductive activation of which is strongly inhibited by NADP<sup>+</sup>. We therefore compared steady state activity to total capacity (Figure 2D) to determine the activation state of NADP-MDH (Figure 2E) in plants with altered FNR contents. This experiment showed significantly lower NADP-MDH activation in *fnr1* plants, and significantly elevated NADP-MDH activation state in *ZmFNR1* plants, confirming that redox poise of the NADP(H) pool does indeed correlate with the NADP<sup>+</sup> photoreduction capacity of the thylakoids. This also demonstrates that in Arabidopsis the abundance and activity of NADP-MDH is regulated to partly counteract the change in NADP<sup>+</sup> photoreduction capacity. These data are in good agreement with work on tobacco FNR-antisense plants showing that the NADP<sup>+</sup>/NADPH ratio is increased (Hajirezaei et al., 2002). It also confirms the findings of Lintala et al. (2014), who showed that in *tic62/tol* double mutant plants lacking both FNR-membrane tethers, NADP<sup>+</sup>/NADPH ratios were increased and the activation state of NADP-MDH decreased (Lintala et al., 2014), indicating that FNR localization is critical to NADP<sup>+</sup> redox poise.

### **FNR contents correlate with glutathione redox state**

Altered NADP(H) redox poise likely impacts on the redox state of the entire chloroplast, and we therefore investigated redox poisoning mechanisms in plants with altered FNR content. GR reduction of glutathione (GSSG to 2xGSH) in the chloroplast is dependent on NADPH (Mittler et al., 2004; Foyer and Noctor, 2011). We investigated the impact of FNR content and location on total and oxidized amounts of glutathione in plant leaves. In this experiment we also examined the impact of FNR localization in more detail: in addition to *ZmFNR1* expressing plants, plants expressing *ZmFNR3*, which is nearly all soluble (Twachtmann et al., 2012) were analysed. Both total and oxidized leaf glutathione are significantly elevated in the *fnr1* mutant (Figure 3A), and the redox poise of glutathione is more oxidized (Figure 3B). Expression of both maize FNR genes results in a decrease in total glutathione (Figure 3A), and in the proportion of oxidized glutathione (Figure 3B). This is only statistically significant in the *ZmFNR1*-expressing lines, indicating that membrane-bound FNR might affect glutathione reduction more strongly than soluble FNR.

### **Thylakoid-bound FNR activity decreases superoxide radical production in the light**

In the reduced state Fd is capable of electron donation to  $O_2$ , generating  $O_2^{\cdot-}$  (Misra and Fridovich, 1971) and inefficient Fd oxidation might lead to longer lifetimes for  $Fd^{red}$ , and greater  $O_2^{\cdot-}$  production. To test this hypothesis, we measured light-dependent  $O_2^{\cdot-}$  production by thylakoid membranes (identical to those used in Figure 2) using electron paramagnetic resonance (EPR). This semi-*in vitro* system was used because intact chloroplasts contain SOD, which has an extremely high rate constant of  $O_2^{\cdot-}$  dismutation, complicating accurate quantitation of  $O_2^{\cdot-}$ . The PET chain was reconstituted by addition of Fd and  $NADP^+$ . Figure 4A and B show light-dependent thylakoid  $O_2^{\cdot-}$  generation using the  $O_2^{\cdot-}$  detector 1-hydroxy-4-isobutyramido-2,2,6,6-tetramethylpiperidinium (TMT-H), which can react with  $O_2^{\cdot-}$  in both soluble and membrane phases (Kozuleva et al., 2011; Kozuleva et al., 2015). Addition of SOD to the suspension, eliminating soluble  $O_2^{\cdot-}$ , allowed dissection of free radical generation by membrane bound and soluble pathways.

Figure 4B shows that when Fd is added to illuminated membranes there is a significant increase in soluble  $O_2^{\cdot-}$  production, as the number of reduced FeS centers at the acceptor side of PSI increases. The further addition of saturating concentrations of  $NADP^+$  caused a significant decrease in soluble  $O_2^{\cdot-}$  generation. Intermembrane  $O_2^{\cdot-}$  production, presumably resulting from  $O_2$  reduction by plastoquinone at PSI (Kozuleva et al., 2014), was unaffected by addition of FNR substrates. This finding is consistent with previous work on illuminated pea thylakoids (Kozuleva and Ivanov, 2010) where  $NADP^+$  suppressed  $O_2$  reduction by Fd, but not by membrane-bound components.

We then examined  $O_2^{\cdot-}$  production in thylakoids isolated from different genotypes (Figure 4C). For comparison the experiment presented in Figure 4C used the same thylakoids as the electron transport measurements in Figure 2. As expected, the addition of  $NADP^+$  to *fnr1* thylakoids has very little impact on  $O_2^{\cdot-}$  generation from  $Fd^{red}$  in the light. In planta, *fnr1* chloroplasts will contain alternative sinks for  $Fd^{red}$ , including soluble native FNR (AtFNR2), and this will presumably alleviate  $O_2^{\cdot-}$  production by electron transfer to  $NADP^+$  from  $Fd^{red}$  to some extent. Total rates of  $O_2^{\cdot-}$  generation from *ZmFNR1* thylakoids in the presence of  $NADP^+$  are lower than in the wt, probably due to a shorter lifetime of  $Fd^{red}$ , and therefore decreased rates of  $O_2^{\cdot-}$  generation from  $Fd^{red}$ . This correlates with the higher rate of  $NADP^+$  photoreduction by *ZmFNR1* thylakoids (Figure 2).

### **Excess soluble FNR increases superoxide radical production in the light**

The data in Figure 4C indicate that membrane bound FNR is capable of quenching  $O_2^{\cdot-}$  production by decreasing the dwell-time of electrons on Fd and passing electrons to stromal sinks. To test whether the addition of soluble FNR could compensate for the loss of membrane-bound FNR in *fnr1* thylakoids, we challenged the thylakoid  $O_2^{\cdot-}$  detection system



with soluble FNR. We previously calculated that maize chloroplasts contain approximately 30  $\mu\text{M}$  FNR in the combined soluble and membrane fractions (Okutani et al., 2005). In Arabidopsis, the proportion of soluble FNR is between 25%-50% in wt plants (Hanke et al., 2005; Benz et al., 2009). We therefore added a soluble, recombinant ZmFNR3 concentration of approximately the same order (5  $\mu\text{M}$ ) to *fnr1* thylakoids, and illuminated in the presence and absence of NADP<sup>+</sup> (Figure 5). Surprisingly, addition of soluble FNR to the system resulted in a dramatic increase in O<sub>2</sub><sup>-</sup> production, and this was partly ameliorated by the omission of NADP<sup>+</sup>.

### **Altered FNR content impacts on ROS and redox perception by the plant.**

It is well documented that signals originating from both glutathione redox poise and O<sub>2</sub><sup>-</sup> influence gene expression (Mehta et al., 1992; Wagner et al., 2004; Mhamdi et al., 2010). To determine whether the FNR dependent changes to *in vitro* free radical generation (Figures 4 and 5) also occur *in planta*, we tested transcript abundance of classical markers responding to general and O<sub>2</sub><sup>-</sup>-specific oxidative stress (*At2g21640* and *DIR5* respectively, Mehterov et al., 2012) and chloroplast redox poise (*NADP-MDH*) (Scheibe et al., 2005; Hameister et al., 2007) by real time quantitative RT-PCR (qRT-PCR). In addition, we selected genes which could potentially be connected to both FNR and redox poise, by interrogating databases of microarray and RNAseq data (see Supplemental Table S2 for details). We selected five genes that are upregulated in arrays comparing *fnr1* mutants with wt, which also showed upregulation in conditions expected to impact on redox metabolism: *WRKY53*, *WRKY70*, *LEA5/SAG21*, *ACD6* and *SYP122*. Transcript abundance of these genes was compared between wt, the *fnr1* mutant, and two lines each over-expressing ZmFNR1 and ZmFNR3, respectively by qRT-PCR (Figure 6). The two stress marker genes (*DIR5* and *At2g21640*) and *NADP-MDH* have wt expression levels in *fnr1*. Apart from *ACD6*, transcripts of all genes potentially responding to both FNR loss and ROS or redox perturbation are increased in *fnr1*, although only *SAG21* and *SYP122* are statistically significant. FNR over-expressing plants also showed increased expression of these genes, although the amplitude of this change varies between lines. In contrast to *fnr1*, markers for both general and O<sub>2</sub><sup>-</sup>-specific oxidative stress are also upregulated in the overexpressors.

Finally, *NADP-MDH* transcripts were significantly increased in all ZmFNR-overexpressing lines, consistent with its role in the malate valve, exporting reducing equivalents to the cytosol when the NADP<sup>+</sup>/NADPH poise is excessively reduced (Scheibe, 2004). Although the correlation between FNR content and activation state of NADP-MDH is consistent between Arabidopsis (Figure 2) and tobacco (Hajirezaei et al., 2002), this is not the case for total enzyme capacity. FNR over-expression in tobacco has no impact, while in tobacco *fnr* antisense lines NADP-MDH activity increases (Scheibe and Dietz, 2012). By contrast, in

Arabidopsis we found that knock out of 50% FNR had no effect on total NADP-MDH activity while over-expression of FNR leads to an increased NADP-MDH transcript (Figure 4). Total activity also increases on FNR over-expression, but this is not statistically significant (Figure 2). The reasons for this difference between species are unclear but the signals leading to upregulation of the NADP-MDH gene are poorly understood. Results in *fnr* antisense tobacco were interpreted as a response to an excessively reduced stroma (Scheibe and Dietz, 2012), and it may be that relative light intensity or photoperiod play a role. Indeed, transcript and protein of the single copy NADP-MDH gene in Arabidopsis only increase in response to high light when plants are grown in short day, but not long day conditions (Becker et al., 2006). No consistent difference in transcripts was observed between *ZmFNR1* and *ZmFNR3* expressing lines. In general, stronger responses were seen in *ZmFNR1-2* and *ZmFNR3-3* than in *ZmFNR1-5* and *ZmFNR3-5*.

There are several reports correlating FNR content with tolerance to high light and other oxidative stresses (Palatnik et al., 2003; Rodriguez et al., 2007; Lintala et al., 2012) and data in Figures 4, 5 and 6 indicate that increasing or decreasing FNR content alters ROS production and perception. We therefore compared the high light susceptibility of genotypes with altered FNR abundance and location (Figure 7). In this experiment, high-light treatment of the *fnr1* mutant did not result in significantly more membrane damage (measured as ion leakage) or damage to PSII (measured as  $\Phi$ II), which is a major site of  $O_2^{\cdot-}$  action (Krieger-Liszka et al., 2011). By contrast, both lines expressing *ZmFNR1* appear partially protected, with significantly less PSII damage and membrane leakage, especially after a short, 1.5 h illumination. This protective effect is less pronounced for *ZmFNR3*-expressing plants, with only  $\Phi$ II being significantly improved relative to the wt.

## DISCUSSION

Data presented in this study show that changes in FNR abundance and localization produce at least two distinct outcomes that are potentially relevant to plant stress tolerance: Firstly, the efficiency of  $NADP^+$  photoreduction has an impact on electron supply to ROS removal pathways. Secondly, altered free radical production, caused by either decreased or increased FNR can induce changes in gene transcription related to stress tolerance.

### A long $Fd^{red}$ half-life could result in $O_2^{\cdot-}$ production

Figure 1 highlights the role of FNR in connecting the ( $Fd^{red}/Fd + e^-$ ) and ( $NADPH/NADP^+ + H^+ + 2e^-$ ) redox couples. *In vitro*, uncoupling these pools leads to a longer half-life for  $Fd^{red}$ , resulting in increased  $O_2^{\cdot-}$  production (*fnr1* in Figure 4). However, under steady state conditions we did not detect upregulation of specifically  $O_2^{\cdot-}$  responsive genes in *fnr1* (Figure 4), and staining for ROS in the tobacco knock-downs detected a specific increase in  $^1O_2$  but

not  $O_2^{\cdot-}$  (Palatnik et al., 2003). Therefore, under steady state conditions other electron acceptors probably quench  $O_2^{\cdot-}$  generation from  $Fd^{red}$ . Despite this, a prolonged  $Fd^{red}$  half-life might be expected in specific conditions, and it is known that plants drastically decrease Fd contents under various stresses (Giro et al., 2006; Tognetti et al., 2006; Liu et al., 2013). Data in Figure 4 indicate that this could be because it is preferable to have charge recombination within PSI than low turnover of  $Fd^{red}$ . Indeed, Arabidopsis mutants lacking the main Fd iso-protein, Fd2, are more tolerant of extended high-light treatment (Liu et al., 2013). The authors attribute this to increased photosynthetic cyclic electron flow, but decreased  $O_2^{\cdot-}$  production could also play a role. In our experiments we did not detect greater susceptibility of Arabidopsis *fnr1* mutants to high-light stress (Figure 7), but Lintala et al. (2009) found that both *fnr1* mutants and *fnr2* knock-downs were more susceptible to MV-induced oxidative stress at room temperature. Decreased FNR is also known to increase susceptibility to photo-oxidative stress in tobacco (Palatnik et al., 2003).

### **Increased soluble FNR results in $O_2^{\cdot-}$ production**

By contrast, increased membrane-bound FNR in the thylakoid system appears to improve coupling between the  $Fd:Fd^{red}$  and  $NADP^+:NADPH$  pools, with less flux to  $O_2^{\cdot-}$  in the presence of a  $NADP^+$  sink *in vitro* (Figure 4), and a more reduced  $NADP(H)$  pool (Figure 2), leading to a more reduced glutathione pool *in planta* (Figure 3). *ZmFNR1* plants and, to a lesser extent *ZmFNR3* plants, appear to be more tolerant to high-light treatment (Figure 7), in line with a previous work in tobacco (Rodriguez et al., 2007). Surprisingly, when we attempted to rescue  $O_2^{\cdot-}$  production in *fnr1* thylakoids by the addition of soluble FNR, we measured a dramatic increase in  $O_2^{\cdot-}$  evolution (Figure 5). Interestingly, other studies on illuminated thylakoids report that addition of several flavoenzymes, including FNR, cause an increase in  $O_2$  consumption (Goetze and Carpentier, 1993; Miyake et al., 1998). Although monodehydroascorbate reductase was identified as the most efficient  $O_2^{\cdot-}$  catalyst, FNR showed half the maximum rate at  $\sim 1.5 \mu M$  enzyme concentrations, still well below the total FNR concentration estimated for the chloroplast of  $\sim 30 \mu M$  (Okutani et al., 2005). Miyake et al. (1998) also report that this activity was independent of Fd, implying that FNR received electrons directly from PSI. By contrast, we measured maximum rates of  $O_2^{\cdot-}$  formation in the presence of  $NADP^+$ , indicating turnover of the enzyme contributes. There are two possible explanations for this result. Firstly, we cannot discount the possibility that excess FNR catalyzes backflow of electrons from photoreduced NADPH to Fd, which in turn reduces  $O_2$ , during the sampling and EPR measurement time. However, this seems unlikely because the higher FNR content of *ZmFNR1* thylakoids does not drive greater  $O_2^{\cdot-}$  production (Figure 4C).

Alternatively,  $O_2^{\cdot-}$  may be generated at FNR. In our system PSI:Fd:FNR is altered from the *in vivo* ratio of 1:5:3 (Bohme, 1978). To minimize shading we used 33  $\mu\text{g}$  chlorophyll  $\text{ml}^{-1}$ , and assuming a chlorophyll:PSI ratio of 600:1 (Kohorn et al., 1992) this gives a PSI:Fd:FNR of  $\sim 1:80:80$ . Under these conditions, one  $\text{Fd}^{\text{red}}$  will pass an electron to one FNR, forming a semiquinone on the FAD until a second  $\text{Fd}^{\text{red}}$  allows completion of the catalytic cycle and reduction of  $\text{NADP}^+$ . Limited electron supply from PSI would therefore extend the life-time of this unstable semiquinone before the second reduction, leading to increased electron donation to  $O_2$  from the semiquinone. Production of  $O_2^{\cdot-}$  by the FAD semiquinone radical of FNR is supported by a study from Bes et al. (1995), who report that while FNR is a poor electron donor to  $O_2$  when the FAD is fully reduced by NADPH, cross-linking FNR to a viologen molecule (which as a single electron carrier would generate a semiquinone at the FAD) converts the enzyme to an efficient NADPH oxidase, (Bes et al., 1995). The ratio of PSI:Fd:FNR therefore seems critical to minimize  $O_2^{\cdot-}$  production during PET.

Interestingly, a spin trapping study on  $O_2^{\cdot-}$  generation by chloroplasts found that the *trf* mutant, which lacks an FNR-membrane tether and has decreased FNR at the membrane, also shows decreased  $O_2^{\cdot-}$  evolution (Vojta et al., 2015). As this difference is also seen on addition of methyl viologen, it is presumably unrelated to the photoreduction of FNR via Fd that we have measured with isolated thylakoids. Rather, the use of intact chloroplasts by Vojta et al., with theoretically intact ROS quenching mechanisms, indicates that an alternative quenching mechanism might be responsible.

### **FNR mutants and over-expressors both show gene expression responses associated with oxidative stress under ambient conditions**

Increased  $O_2^{\cdot-}$  on perturbation of FNR content should be detectable at the level of gene expression, where many ROS markers have been identified (Mehta et al., 1992; Wagner et al., 2004). We selected markers for general oxidative stress,  $O_2^{\cdot-}$ -specific stress (*At2g21640* and *DIR5*, respectively) and genes potentially upregulated in response to both *FNR* loss and ROS or redox perturbation (Supplemental Table S2): expression of the *WRKY70* transcription factor is induced by ROS (Brosche et al., 2014) and red light (Joo et al., 2005), and the protein counteracts cell death during senescence and plant defense by inducing a salicylic acid (SA) response and suppressing a JA response (Li et al., 2004; Li et al., 2006; Ulker et al., 2007; Shim et al., 2013); *WRKY53* is highly induced by  $\text{H}_2\text{O}_2$  and acts antagonistically to *WRKY70*, accelerating cell death during senescence and defense (Besseau et al., 2012); *SAG21* is another senescence-associated gene whose expression is triggered by  $\text{H}_2\text{O}_2$  and  $O_2^{\cdot-}$  (Salleh et al., 2012), and is reported to confer tolerance to oxidative stress in yeast (Mowla et al., 2006). *ACD6*, and *SYP122* are additional components of the SA-signaling network initiated

during defense (Lu et al., 2003; Zhang et al., 2007; Zhang et al., 2008; Tateda et al., 2015). Interestingly, both *WRKY53* and *SAG21* were also found to be upregulated in *trp1* mutants (Juric et al., 2009). Unexpectedly, qRT-PCR indicates that mRNAs of these genes are increased not only in *fnr1*, but also in both *ZmFNR1*- and *ZmFNR3*-expressing plants, which additionally show upregulation of oxidative stress and  $O_2^{\cdot-}$ -specific markers (Figure 6). This finding opens up the intriguing possibility that the protection against oxidative stress in FNR over-expressing plants might be partly due to systemic acquired acclimation (Rao et al., 1997), with plants “primed” by  $O_2^{\cdot-}$  generated under growth-light conditions pre-inducing oxidative stress protection. This may partly explain their increased tolerance to high-light stress (Figure 7). Critically, although *fnr1* plants do show increased expression of some genes that respond to oxidative stress, the specific marker for  $O_2^{\cdot-}$  is not upregulated (Figure 6), consistent with a lack of priming and a failure to increase high light tolerance (Figure 7).

### **Relative contributions of membrane bound and soluble FNR**

*In vitro* measurements allowed us to dissect the impact of increased membrane bound FNR, which results in lower  $O_2^{\cdot-}$  production (Figure 4C) from increased soluble FNR, which resulted in increased  $O_2^{\cdot-}$  production (Figure 5). However, expression of both membrane bound and soluble FNR resulted in perception of  $O_2^{\cdot-}$  at the level of gene expression (Figure 6) and improved high light tolerance (Figure 7). All FNR expressing lines also contain native FNRs in both soluble and membrane bound locations and so the results indicate that total FNR content may be more critical than localization under these growth conditions. However, plants expressing membrane bound FNR have a more reduced glutathione pool (Figure 3), and were slightly more tolerant to high light stress than those expressing soluble FNR (Figure 7). In combination with the observation that *fnr2* plants (which have membrane bound FNR) are more stress tolerant than *fnr1* plants (which have only soluble FNR) at low temperature (Lintala et al., 2009), this supports a greater role for membrane bound FNR in stress tolerance.

### **Metabolic impact of FNR on redox poise and stress tolerance**

FNR contents, in particular of membrane-bound FNR, correlate with glutathione redox poise (Figure 3) and activation state of the NADP-MDH, which is a readout of  $NADP^+/NADPH$  redox poise (Figure 2). Based on these data, we propose that the velocity of NADPH regeneration may be translated to the redox poise of chloroplast glutathione. This has previously been reported for the cytosol, where inhibition of the oxidative pentose phosphate pathway prevents  $NADP^+$  reduction, resulting in a more oxidized glutathione pool (Mou et al., 2003). However, the changes in glutathione redox poise seen in Figure 3 are unlikely to result in altered ascorbate regeneration, because the ascorbate:DHAR redox couple has a much more positive redox potential than the GSH/GSSG redox couple (Foyer and Noctor, 2011) and will therefore

remain predominantly reduced even when the majority of glutathione is oxidized. For this reason, differences in ascorbate regeneration can probably be discounted as the cause of altered stress tolerance of *fnr1* and *ZmFNR1* plants (Figure 7). Alternatively, altered glutathione redox poise in *fnr1* and *ZmFNR* lines might influence signaling cascades originating in cytosolic glutathione (Chen and Dickman, 2004; Mhamdi et al., 2010). Oxidized cytosolic glutathione can be transported into the vacuole (Queval et al., 2011) and the chloroplast membrane contains glutathione transporters (Maughan et al., 2010), suggesting that chloroplast glutathione redox poise might also be transmitted to the cytosol. Indeed, WRKY53 has been shown to interact with a glutathione S-transferase in a yeast 2-hybrid screen (Van Eck et al., 2014), providing a link between glutathione redox poise and genes with increased transcript in both *fnr1* and *ZmFNR* lines (Figure 6).

Finally, altered FNR activity might also impact on the metabolic capacity of the cell to dissipate oxidative stress. For example, disturbed NADPH/NADP<sup>+</sup> ratios could result in altered electron supply, not only to GR, but also other NADPH-dependent enzymes involved in stress response, such as chloroplast alkenal/one oxidoreductase (Yamauchi et al., 2012). As highlighted in Figure 1, chloroplast stress relief enzymes are supported by both Fd- and NADPH-reduction systems. The correlation between FNR content and stress tolerance might reflect the capacity to interconvert Fd and NADPH, allowing the plant to rapidly exploit both Fd-dependent and NADPH-dependent ROS removal and regulatory mechanisms in the chloroplast (Asada, 1999; Hanke et al., 2009; Foyer and Noctor, 2011).

In summary, our work indicates that the ratio between components at the end of the linear electron transport chain is critical to efficiently couple the Fd/Fd<sup>red</sup> and NADP<sup>+</sup>/NADPH redox pools, prevent superoxide generation, and balance the chloroplast redox poise. The resultant disturbances in chloroplast and glutathione redox poise, and in ROS perception will influence the plant's investment in either photosynthetic apparatus, or stress response machinery, and therefore affect growth efficiency. This provides an example of how fine tuning the ratio of specific PET chain components can induce a stress acclimation response.

## **METHODS**

### **Plant Growth, Chloroplast Isolation and Thylakoid Preparation**

Unless otherwise indicated, plants were grown in 10 h light at 21°C, 14 h dark at 18°C. Chloroplast preparation for electron transport and EPR measurements with thylakoid membranes was basically as described previously (Hanke et al., 2008). Genotypes wt Col and *fnr1* were as described previously (Hanke et al., 2008), maize *FNR1* and *FNR3* over-expressing plants were as described previously (Twachtmann et al., 2012). Plants for high-light treatment were germinated under Lumilux cool white lights (Osram FQ, Germany) at 150

$\mu\text{E s}^{-1} \text{m}^{-2}$  and transferred to growth chambers with SON-T Agro lamps (Phillips, Eindhoven, The Netherlands) at the same light intensity 1 week before high-light treatment at  $600 \mu\text{E s}^{-1} \text{m}^{-2}$  under SON-T Agro lamps.

### **Measurements of Electron Transfer Activity in Isolated Thylakoids**

Total electron transfer capacity of thylakoids was measured as electron flux to  $[\text{Fe}(\text{CN})_6]^{3-}$  on illumination with light above 610 nm (cut-off filter) at  $600 \mu\text{E m}^{-2} \text{s}^{-1}$  in a 1 mm light path cuvette. Reactions contained thylakoids at a final chlorophyll concentration of  $33 \mu\text{g ml}^{-1}$ , 330 mM sorbitol, 50 mM HEPES, 20 mM NaCl, 5 mM  $\text{MgCl}_2$ , 0.1  $\mu\text{M}$  nigericin and 500  $\mu\text{M}$   $[\text{Fe}(\text{CN})_6]^{3-}$ . Absorbance difference between 420 nm and 540 nm was measured after 0, 0.5, 1, 2 and 5 min illumination to calculate the rate. NADP<sup>+</sup> photoreduction was measured in an identical system, substituting 5  $\mu\text{M}$  Arabidopsis Fd2 and 200  $\mu\text{M}$  NADP<sup>+</sup> for  $[\text{Fe}(\text{CN})_6]^{3-}$ , and following the change in absorbance difference between 340 nm and 390 nm. Total FNR activity was measured in the supernatant following a 0.1% Triton X-100 wash of thylakoid membranes to remove all peripheral proteins. The reaction was followed in a cytochrome c reduction assay as described previously (Hanke et al., 2004) in the presence of a 10  $\mu\text{M}$  concentration of Arabidopsis Fd2 (purified as described by Hanke et al., 2004).

### **Determination of NADP-MDH Activation State**

Measurements were performed basically as described previously (Scheibe and Stitt, 1988). In brief, leaf material was rapidly sandwiched between two sheets of solid  $\text{CO}_2$  before grinding in liquid nitrogen avoiding any shading prior to freeze-clamp. All following steps were performed in degassed buffers under  $\text{N}_2$ . Protein was extracted into 50 mM HEPES pH 6, 2 mM EDTA, 2 mM DTT, 1 mM Pefabloc, 0.1% BSA and 0.1% Triton X-100 to maintain *in situ* activity, and enzyme activity was measured in 100 mM Tris-HCl pH 8, 1 mM EDTA, 0.1% BSA, 0.2 mM NADPH. Reactions were started by addition of 1 mM oxaloacetic acid, and rates were followed at 340 nm. Rates were corrected for non-specific NADP-dependent activity of the more abundant NAD-MDH (0.2% of the NAD-dependent rate was assumed to be due to the non-specific NADP-dependent activity; NAD-MDH activity was measured at a higher extract dilution by addition of NADH rather than NADPH) (Scheibe and Stitt, 1988). Total activity was established by enzyme activation at room temperature in activation buffer: 200 mM Tris-HCl pH 8.4, 1 mM EDTA, 1 mM Pefabloc, 1 % BSA, 100 mM DTT. Activity was measured at 0, 10, 20 and 40 min to confirm a plateau of maximum activity.

### **Total and Oxidized Glutathione Measurements**

Metabolite assays were performed on mature leaf tissue from 6-8 week old plants. Tissue was always harvested under growth lights by grinding in liquid nitrogen. The assays for total and oxidized glutathione were performed with the glutathione (total), detection kit from Enzo Life

Sciences (Lörrach, Germany) according to the manufacturer's instructions, except for measurement of oxidized glutathione, where 20 mM 2-vinylpyridine rather than 4-vinylpyridine was used to block free thiol sites.

### **EPR Spectroscopy for superoxide detection**

Reactions were assembled at low light ( $< 1 \mu\text{E s}^{-1} \text{m}^{-2}$ ) in a quartz cuvette in a volume of 150  $\mu\text{l}$  containing thylakoids ( $33 \mu\text{g chlorophyll ml}^{-1}$ ), 330 mM sorbitol, 50 mM HEPES-NaOH (pH 7.5), 1 mM  $\text{MgCl}_2$ , 50  $\mu\text{M}$  deferoxamine mesilate, 0.1  $\mu\text{M}$  nigericin, and 3.3  $\mu\text{M}$  1-hydroxy-4-isobutyramido-2,2,6,6-tetramethylpiperidinium (TMT-H) (Kozuleva et al., 2011) unless otherwise specified. Aliquots of 20  $\mu\text{l}$  were taken for the EPR measurements. Light treatments were at  $600 \mu\text{E s}^{-1} \text{m}^{-2}$  for 2 min at  $21^\circ\text{C}$ , using a 100 W halogen lamp unless otherwise stated. To prevent unwanted radical formation from the spin trap by UV radiation, a cut-off filter removing wavelengths below 610 nm was used. EPR measurements were performed at room temperature (296–299 K) with a home-made X-band EPR spectrometer equipped with a Bruker dielectric resonator or on a Miniscope X-band benchtop EPR spectrometer (MS200; Magnettech GmbH, Berlin, Germany) equipped with a rectangular TE102 resonator, with the microwave power set to 0.4–0.6 mW and B-field modulation amplitude adjusted to 0.15 mT. Samples were measured in EPR glass capillaries (0.9 mm inner diameter).

The  $\text{O}_2^{\cdot-}$  radical concentration was calculated using a standard solution of the stable nitroxide radical TEMPOL at a known concentration. In order to distinguish soluble superoxide radical generation from radical production within the thylakoid membrane, superoxide dismutase (200  $\text{U ml}^{-1}$ ) was added to the suspension. The total rate of  $\text{O}_2^{\cdot-}$  generation was equal to the rate of nitroxide radical accumulation in the absence of SOD. The rate of soluble ("stromal")  $\text{O}_2^{\cdot-}$  generation was calculated by subtracting the rate of nitroxide radical accumulation in the presence of SOD (+SOD) from the total rate (-SOD).

Recombinant maize FNR3 was prepared as describe previously (Okutani et al., 2005).

### **Quantitative Real-Time PCR**

Total RNA was isolated from 100 mg frozen leaf material by using PureLink® RNA Mini Kit (Ambion, Thermo Fisher Scientific, Darmstadt, Germany) as per the manufacturer's protocol, with some additional modifications. After RNA isolation, DNase digestion was performed to remove genomic DNA using TURBO DNA-free™ Kit (Ambion, Thermo Fisher Scientific, Darmstadt, Germany). The method was performed according to the manufacturer's instructions. After RNA isolation and DNase treatment, samples were analyzed by qPCR to test for contamination with genomic DNA using intron-specific primers (Supplemental Table S3). Afterwards, cDNA was synthesized from 2  $\mu\text{g}$  total RNA using oligo(dT) as primers



according to the manufacturer's instructions (Fermentas RevertAid™ First Strand cDNA Synthesis Kit, Fermentas GmbH, St. Leon-Rot, Germany).

Quantitative real-time PCR was performed as described previously (Karpinski et al., 1999). Briefly, all primers were tested for their precise annealing temperature and efficiency before use. A PCR assay efficiency range from 90% to 110% was considered acceptable. Thereafter, only primers exhibiting this efficiency were used and are shown in Supplemental Table S3. Real-time PCR was performed using a Thermal Cycler (C1000™, Biorad, München) and a real-time system (CFX96™, Biorad, München). All transcripts were normalized to the housekeeping gene *RAN3*.

### **Chlorophyll Fluorescence and Membrane Leakage**

Measurements were performed on 1 cm diameter leaf discs cut from mature leaves of 6-8 week old plants. Leaf discs were floated on 4 ml MilliQ water before high-light treatment. Ion leakage was detected as conductivity of the water solution measured with an electrode (Hannah Instruments, Kehl am Rhein, Germany) and fluorescence of leaf discs was measured using a FluorCam (Photon Systems Instruments, Brno, Czech Republic). Photosystem II capacity ( $\Phi_{II}$ ) was calculated following 10 min dark adaptation, as  $F_V$  (variable fluorescence after dark adaptation) /  $F_M$  (maximal fluorescence after dark adaptation).

### **Accession Numbers**

Sequence data from this article can be found in the Arabidopsis Genome Initiative or GenBank/EMBL databases under the following accession numbers: maize FNR1, BAA88236; FNR3, ACF85815; *Arabidopsis* FNR1, AT5G66190; FNR2, AT1G20020; WRKY53, AT4G23810; WRKY70, AT3G56400; LEA5/SAG21, AT4G02380; ACD6, AT4G14400; SYP122, AT3G52400; RAN3, AT5G55190.

### **Supplemental Material**

**Supplemental Figure S1.** Response of Arabidopsis plants with different FNR contents to high light treatment (original data).

**Supplemental Table S1.** Rates of NADP-MDH activity in crude protein extracts of Arabidopsis leaves.

**Supplemental Table S2.** Rationale for the selection of genes investigated by qRT-PCR in Figure 6.

**Supplemental Table S3.** Primers used in cDNA quality control and qRT-PCR.

## Figure Legends

**Figure 1.** FNR plays a central role in chloroplast redox metabolism. Simplified diagram of chloroplast redox metabolism related to the transfer of electrons between the ferredoxin redox couple ( $\text{Fd}^{\text{red}} / \text{Fd} + \text{e}^-$ ) and the NADP(H) redox couple ( $\text{NADPH} / \text{NADP}^+ + \text{H}^+ + 2\text{e}^-$ ) by the enzyme FNR. Photosynthetic electron transport (PET) reduces Fd to  $\text{Fd}^{\text{red}}$ , and both PET and  $\text{Fd}^{\text{red}}$  are sources of superoxide ( $\text{O}_2^{\cdot-}$ ). There are many Fd-dependent enzymes, including essential components of bioassimilation and biosynthesis (Hanke and Mulo, 2013) and the ferredoxin:thioredoxin reductase (FTR), which reduces thioredoxin (Trx), transducing a redox signal to regulate many chloroplast enzymes (Schurmann and Buchanan, 2008). The majority of  $\text{Fd}^{\text{red}}$  is oxidized by the enzyme FNR to reduce  $\text{NADP}^+$  to NADPH.  $\text{NADP}^+$  is regenerated by many enzymes, including other proteins involved in biosynthesis and bioassimilation and the NADPH-dependent Trx reductase C (NTRC), which also reduces thiol groups, resulting in a redox signal and supports antioxidant metabolism by regenerating 2-Cys peroxiredoxin (Dietz et al., 2002). When the redox poise of the NADP(H) pool is too reduced,  $\text{NADP}^+$  can be regenerated by the NADP-malate dehydrogenase (NADP-MDH), and operation of the malate valve to export reducing equivalents from the chloroplast (Backhausen et al., 1994). The  $\text{O}_2^{\cdot-}$  radical is removed in the water-water cycle by the action of first superoxide dismutase (SOD) and then ascorbate peroxidase (APX), resulting in oxidation of ascorbate to dehydroascorbate (Foyer and Halliwell, 1976; Groden and Beck, 1979; Asada, 1999). Reductive regeneration of ascorbate can be supported directly by  $\text{Fd}^{\text{red}}$ , or through glutathione (GSH) oxidation to GSSG by dehydroascorbate reductase (DHAR). GSH regeneration is supported in turn by NADPH, through action of glutathione reductase (GR). Thus both  $\text{Fd}^{\text{red}}$  and FNR are involved in removal of reactive oxygen species (ROS).

**Figure 2.** FNR activity and chloroplast NADP(H) poise is altered in FNR transgenics. A, FNR activity of isolated thylakoid membranes from *Arabidopsis* wt, *fnr1* mutant and two independent lines expressing maize *FNR1*, measured as reduction of cytochrome *c* on addition of NADPH and 10  $\mu\text{M}$  Fd. B, Capacity for light-dependent electron flux from  $\text{H}_2\text{O}$  by isolated thylakoid membranes of the indicated plants, measured as reduction of  $[\text{Fe}(\text{CN})_6]^{3-}$  by PSI on illumination. (C) Light-dependent  $\text{NADP}^+$  photoreduction by isolated thylakoid membranes from the indicated plants, measured as reduction of  $\text{NADP}^+$  by PSI on illumination. A, B and C values are means  $\pm$ s.e. of 3 measurements and typical of two separate experiments. D, Measurement of NADP(H) redox poise. *Arabidopsis* plants with the indicated genotypes were harvested either under growth-light (grey) or dark-adapted (black) conditions. Extracts were used for measurement of steady state NADP-MDH activity. Total enzyme activity (white bars) was determined following incubation of the extract for 40 min in activating buffer (see methods). Values are means  $\pm$  s.e. of 3-6 biological replicates. As dark values are

low to non-detectable, original values are given in Supplemental Table S1 for clarity. E, Percentage activation state of NADP-MDH in the indicated genotypes under steady-state growth-light conditions, calculated for the individuals averaged in part D. Values are means  $\pm$  s.e. of 3-6 biological replicates. Significant differences in of *fnr1* and *FNR1* expressing plants from the wt in a *t*-test for small samples are indicated by \* ( $P < 0.05$ ).

**Figure 3.** Downstream impact of FNR content on redox poise of glutathione. A, Measurement of total glutathione (black) and glutathione in the oxidized state (white) in leaves of wt, *fnr1*, two independent lines expressing *ZmFNR1*, and two independent lines expressing *ZmFNR3*, measured by enzymatic cycling assay. B, Percentage of glutathione in the oxidized state in leaves of wt, *fnr1*, two independent lines expressing *ZmFNR1*, and two independent lines expressing *ZmFNR3*, calculated from the data shown in A. Values are means  $\pm$  s.e. of 3-6 biological replicates. In comparisons with wt, statistical significance in a *t*-test for small samples is indicated by \* ( $p < 0.05$ ), \*\* ( $p < 0.01$ ).

**Figure 4.** Impact of thylakoid FNR content on  $O_2^{\cdot-}$  production. A, Detection of light dependent  $O_2^{\cdot-}$  evolution from purified Arabidopsis thylakoid membranes. Representative electron paramagnetic resonance (EPR) spectra before (black lines) and after (blue lines) illumination. The experiment was performed in the absence (upper panels) and presence (lower panels) of superoxide dismutase (SOD) to remove soluble  $O_2^{\cdot-}$ . B, Left, light-dependent TMT $^{\cdot}$  radical generation by thylakoid membranes, calculated using the spectra shown in part A and two further replicates, in the absence (diagonal stripes) and presence (horizontal stripes) of SOD. In comparisons between - SOD measurements, significant difference from thylakoid only measurements in a *t*-test for small samples is indicated by \* ( $p < 0.05$ ), \*\* ( $p < 0.01$ ). Right, light-dependent soluble  $O_2^{\cdot-}$  evolution by Arabidopsis thylakoid membranes calculated by subtracting +SOD from the -SOD rates shown in the graph on the left. C, Light dependent soluble  $O_2^{\cdot-}$  evolution in thylakoid membranes from the indicated Arabidopsis genotypes, calculated by subtracting the +SOD from the -SOD rates, in the presence of Fd (white bars) or Fd and NADP $^+$  (black bars). Standard deviation of the original data was less than 5% and significant difference from the equivalent wt measurement in a *t*-test for small samples is indicated by \* ( $p < 0.05$ ), \*\* ( $p < 0.01$ ). Experiment was repeated two times with similar results.

**Figure 5.** Impact of additional soluble FNR on superoxide production. Left, light dependent TMT $^{\cdot}$  radical generation by *fnr1* thylakoid membranes illuminated with variable combinations of Fd, NADP $^+$  and soluble FNR in the absence (diagonal stripes) and presence (horizontal stripes) of SOD. In comparisons between - SOD measurements, statistical difference from *fnr1* + Fd + NADP $^+$  in a *t*-test for small samples is indicated by \* ( $p < 0.05$ ), \*\* ( $p < 0.01$ ). Right, light -dependent soluble  $O_2^{\cdot-}$  evolution in Arabidopsis thylakoid membranes, calculated by

subtracting +SOD from the –SOD rates shown in the graph on the left. The experiment was repeated two times with similar results.

**Figure 6.** Transcript abundance of ROS and redox responsive genes in wt, *fnr1* and two independent lines expressing either membrane bound (*ZmFNR1*) or soluble (*ZmFNR3*) FNR. Genes are: a responsive marker for  $O_2^{\cdot-}$ , *DIR5*; a responsive marker for oxidative stress, *At2g21640*; a marker for disturbed NADP(H) poise, *NADP-MDH*; and 5 genes whose transcript is reported to be upregulated both in *fnr1* and in response to ROS or redox perturbation: *WRKY53*, *WRKY70*, *SAG21*, *SYP122* and *ACD6*. Histograms show mean normalized expression (MNE) relative to the housekeeping gene RAN3. RNA was isolated from plants 3 h into the light period in standard growth conditions and qRT-PCR performed with the resulting cDNA. Values are means  $\pm$ s.e. of three biological replicates. Statistical significance, in a t-test is indicated by \* ( $p < 0.05$ ).

**Figure 7.** High light tolerance of *fnr1* and *FNR* over-expressing transgenic plants. High light induced damage to wt (black bars), *fnr1* (white bars), two independent lines over-expressing the membrane bound *ZmFNR1* (horizontal bars) and two independent lines over-expressing the soluble *ZmFNR3* (vertical bars). Leaf discs were excised from the leaves of at least 5 individual plants 1 h into the light period, floated on 3 ml MilliQ water and exposed to 600  $\mu$ E high light stress. Damage was followed by A, measuring PSII capacity ( $\Phi$  II of the leaf discs) and B, membrane leakage (increased conductivity of the MilliQ water) at the indicated time points. The dark bar between 4.5 and 21 h represents an 8 h night period. Data displayed are % of initial values from 5 biological replicates, averages of which are given in Supplemental Figure S1. In comparison with changes in the wt, statistical significance in a t-test for small samples is indicated by \* ( $p < 0.05$ ).

## REFERENCES

- Allen JF, Hall DO** (1974) The relationship of oxygen uptake to electron transport in photosystem I of isolated chloroplasts: the role of superoxide and ascorbate. *Biochem Biophys Res Commun* **58**: 579-585
- Alte F, Stengel A, Benz JP, Petersen E, Soll J, Groll M, Bolter B** (2010) Ferredoxin:NADPH oxidoreductase is recruited to thylakoids by binding to a polyproline type II helix in a pH-dependent manner. *Proc Natl Acad Sci U S A* **107**: 19260-19265
- Andersen B, Scheller HV, Moller BL** (1992) The PSI-E subunit of photosystem I binds ferredoxin:NADP<sup>+</sup> oxidoreductase. *FEBS Lett* **311**: 169-173
- Asada K** (1999) THE WATER-WATER CYCLE IN CHLOROPLASTS: Scavenging of Active Oxygens and Dissipation of Excess Photons. *Annu Rev Plant Physiol Plant Mol Biol* **50**: 601-639
- Backhausen JE, Kitzmann C, Scheibe R** (1994) Competition between electron acceptors in photosynthesis: Regulation of the malate valve during CO<sub>2</sub> fixation and nitrite reduction. *Photosynth Res* **42**: 75-86
- Batie CJ, Kamin H** (1981) The relation of pH and oxidation-reduction potential to the association state of the ferredoxin . ferredoxin:NADP<sup>+</sup> reductase complex. *J Biol Chem* **256**: 7756-7763
- Batie CJ, Kamin H** (1984) Electron transfer by ferredoxin:NADP<sup>+</sup> reductase. Rapid-reaction evidence for participation of a ternary complex. *J Biol Chem* **259**: 11976-11985
- Batie CJ, Kamin H** (1986) Association of ferredoxin-NADP<sup>+</sup> reductase with NADP(H) specificity and oxidation-reduction properties. *J Biol Chem* **261**: 11214-11223
- Becker B, Holtgreffe S, Jung S, Wunrau C, Kandlbinder A, Baier M, Dietz KJ, Backhausen JE, Scheibe R** (2006) Influence of the photoperiod on redox regulation and stress responses in *Arabidopsis thaliana* L. (Heynh.) plants under long- and short-day conditions. *Planta* **224**: 380-393
- Bes MT, De Lacey AL, Peleato ML, Fernandez VM, Gomez-Moreno C** (1995) The covalent linkage of a viologen to a flavoprotein reductase transforms it into an oxidase. *Eur J Biochem* **233**: 593-599
- Benz JP, Stengel A, Lintala M, Lee YH, Weber A, Philippar K, Gugel IL, Kaieda S, Ikegami T, Mulo P, Soll J, Bolter B** (2009) *Arabidopsis* Tic62 and ferredoxin-NADP(H) oxidoreductase form light-regulated complexes that are integrated into the chloroplast redox poise. *Plant Cell* **21**: 3965-3983
- Besseau S, Li J, Palva ET** (2012) WRKY54 and WRKY70 co-operate as negative regulators of leaf senescence in *Arabidopsis thaliana*. *Journal of experimental botany* **63**: 2667-2679
- Bohme H** (1978) Quantitative determination of ferredoxin, ferredoxin-NADP<sup>+</sup> reductase and plastocyanin in spinach chloroplasts. *Eur J Biochem* **83**: 137-141
- Brosche M, Blomster T, Salojarvi J, Cui F, Sipari N, Leppala J, Lamminmaki A, Tomai G, Narayanasamy S, Reddy RA, Keinanen M, Overmyer K, Kangasjarvi J** (2014) Transcriptomics and functional genomics of ROS-induced cell death regulation by RADICAL-INDUCED CELL DEATH1. *PLoS genetics* **10**: e1004112
- Carrillo N, Ceccarelli EA** (2003) Open questions in ferredoxin-NADP<sup>+</sup> reductase catalytic mechanism. *Eur J Biochem* **270**: 1900-1915
- Cassan N, Lagoutte B, Setif P** (2005) Ferredoxin-NADP<sup>+</sup> reductase. Kinetics of electron transfer, transient intermediates, and catalytic activities studied by flash-absorption spectroscopy with isolated photosystem I and ferredoxin. *J Biol Chem* **280**: 25960-25972
- Chen S, Dickman MB** (2004) Bcl-2 family members localize to tobacco chloroplasts and inhibit programmed cell death induced by chloroplast-targeted herbicides. *J Exp Bot* **55**: 2617-2623
- Chew O, Whelan J, Millar AH** (2003) Molecular definition of the ascorbate-glutathione cycle in *Arabidopsis* mitochondria reveals dual targeting of antioxidant defenses in plants. *J Biol Chem* **278**: 46869-46877
- Dietz KJ, Horling F, Konig J, Baier M** (2002) The function of the chloroplast 2-cysteine peroxiredoxin in peroxide detoxification and its regulation. *J Exp Bot* **53**: 1321-1329

- Foyer CH, Halliwell B** (1976) The presence of glutathione and glutathione reductase in chloroplasts: A proposed role in ascorbic acid metabolism. *Planta* **133**: 21-25
- Foyer CH, Noctor G** (2011) Ascorbate and glutathione: the heart of the redox hub. *Plant Physiol* **155**: 2-18
- Giro M, Carrillo N, Krapp AR** (2006) Glucose-6-phosphate dehydrogenase and ferredoxin-NADP(H) reductase contribute to damage repair during the soxRS response of *Escherichia coli*. *Microbiology* **152**: 1119-1128
- Goetze DC, Carpentier R** (1993) Ferredoxin-NADP<sup>+</sup> reductase is the site of oxygen reduction in pseudocyclic electron transport. *Canadian Journal of Botany* **72**: 256-260
- Groden D, Beck E** (1979) H<sub>2</sub>O<sub>2</sub> destruction by ascorbate-dependent systems from chloroplasts. *Biochim Biophys Acta* **546**: 426-435
- Hajirezaei MR, Peisker M, Tschiersch H, Palatnik JF, Valle EM, Carrillo N, Sonnewald U** (2002) Small changes in the activity of chloroplastic NADP(+)-dependent ferredoxin oxidoreductase lead to impaired plant growth and restrict photosynthetic activity of transgenic tobacco plants. *Plant J* **29**: 281-293
- Hameister S, Becker B, Holtgreffe S, Strodtkotter I, Linke V, Backhausen JE, Scheibe R** (2007) Transcriptional regulation of NADP-dependent malate dehydrogenase: comparative genetics and identification of DNA-binding proteins. *Journal of molecular evolution* **65**: 437-455
- Hanke G, Mulo P** (2013) Plant type ferredoxins and ferredoxin-dependent metabolism. *Plant Cell Environ* **36**: 1071-1084
- Hanke GT, Endo T, Satoh F, Hase T** (2008) Altered photosynthetic electron channelling into cyclic electron flow and nitrite assimilation in a mutant of ferredoxin:NADP(H) reductase. *Plant Cell Environ* **31**: 1017-1028
- Hanke GT, Holtgreffe S, König N, Strodkötter I, Voss I, Scheibe R** (2009) Use of Transgenic Plants to Uncover Strategies for Maintenance of Redox Homeostasis During Photosynthesis. *Advances in Botanical Research* **52**: 207-251
- Hanke GT, Kimata-Arigo Y, Taniguchi I, Hase T** (2004) A post genomic characterization of *Arabidopsis* ferredoxins. *Plant Physiology* **134**: 255-264
- Hanke GT, Okutani S, Satomi Y, Takao T, Suzuki A, Hase T** (2005) Multiple iso-proteins of FNR in *Arabidopsis*: evidence for different contributions to chloroplast function and nitrogen assimilation. *Plant, Cell and Environment* **28**: 1146-1157
- Joo JH, Wang S, Chen JG, Jones AM, Fedoroff NV** (2005) Different signaling and cell death roles of heterotrimeric G protein alpha and beta subunits in the *Arabidopsis* oxidative stress response to ozone. *Plant Cell* **17**: 957-970
- Jose Quiles M, Cuello J** (1998) Association of ferredoxin-NADP oxidoreductase with the chloroplastic pyridine nucleotide dehydrogenase complex in barley leaves. *Plant Physiol* **117**: 235-244
- Juric S, Hazler-Pilepic K, Tomasic A, Lepedus H, Jelacic B, Puthiyaveetil S, Bionda T, Vojta L, Allen JF, Schleiff E, Fulgosi H** (2009) Tethering of ferredoxin:NADP<sup>+</sup> oxidoreductase to thylakoid membranes is mediated by novel chloroplast protein TROL. *Plant J* **60**: 783-794
- Karpinski S, Reynolds H, Karpinska B, Wingsle G, Creissen G, Mullineaux P** (1999) Systemic signaling and acclimation in response to excess excitation energy in *Arabidopsis*. *Science* **284**: 654-657
- Kohorn BD, Lane S, Smith TA** (1992) An *Arabidopsis* serine/threonine kinase homologue with an epidermal growth factor repeat selected in yeast for its specificity for a thylakoid membrane protein. *Proc Natl Acad Sci U S A* **89**: 10989-10992
- Konig J, Baier M, Horling F, Kahmann U, Harris G, Schurmann P, Dietz KJ** (2002) The plant-specific function of 2-Cys peroxiredoxin-mediated detoxification of peroxides in the redox-hierarchy of photosynthetic electron flux. *Proc Natl Acad Sci U S A* **99**: 5738-5743
- Kozuleva M, Petrova AA, Mamedov MD, Semenov AY, Ivanov BN** (2014) O<sub>2</sub> reduction by photosystem I involves phylloquinone under steady-state illumination. *FEBS Lett* **588**: 4364-4368

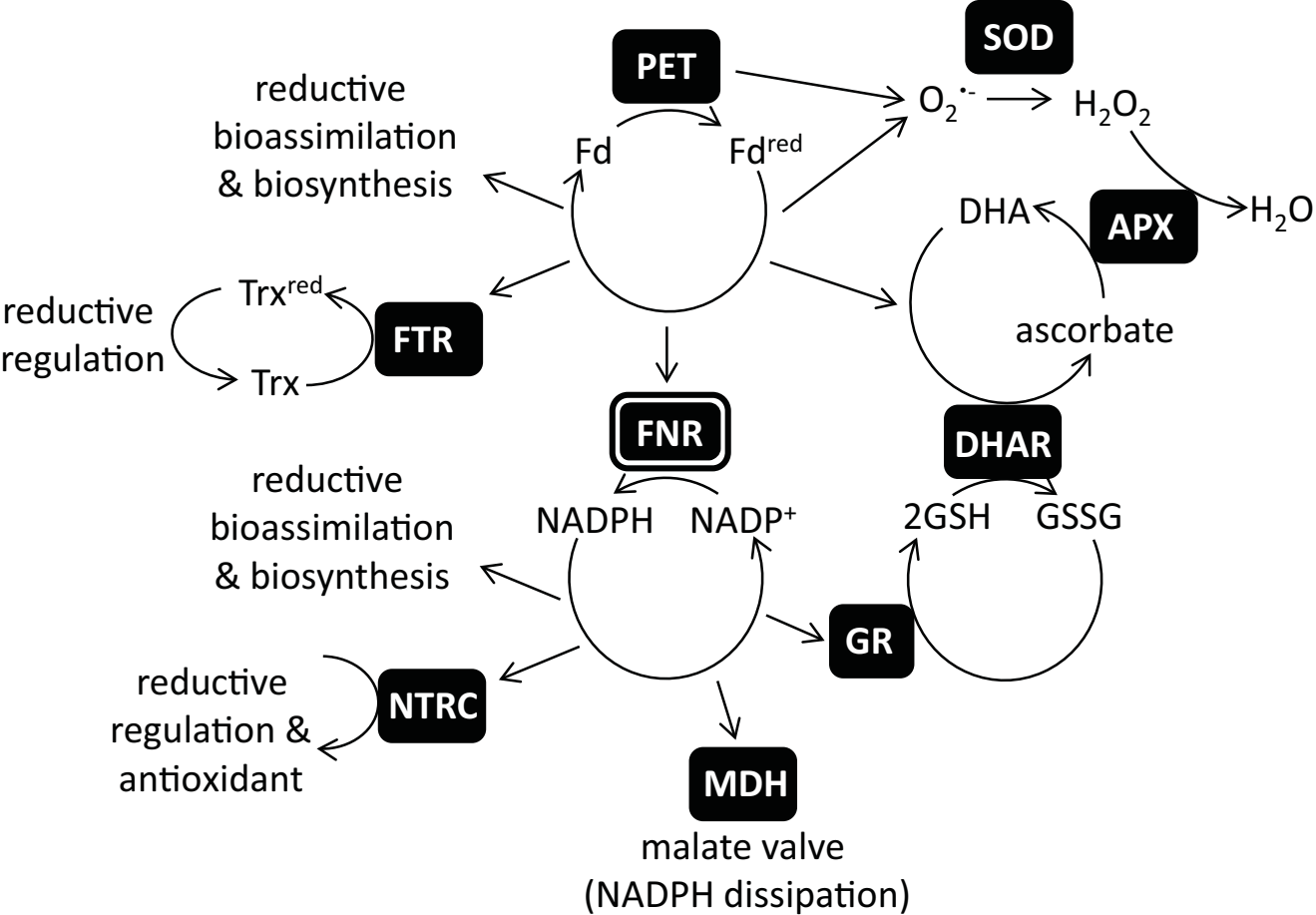
- Kozuleva M, Klenina I, Mysin I, Kirilyuk I, Opanasenko V, Proskuryakov I, Ivanov B** (2015) Quantification of superoxide radical production in thylakoid membrane using cyclic hydroxylamines. *Free Radic Biol Med* **89**: 1014-1023
- Kozuleva M, Klenina I, Proskuryakov I, Kirilyuk I, Ivanov B** (2011) Production of superoxide in chloroplast thylakoid membranes ESR study with cyclic hydroxylamines of different lipophilicity. *FEBS Lett* **585**: 1067-1071
- Kozuleva MA, Ivanov BN** (2010) Evaluation of the participation of ferredoxin in oxygen reduction in the photosynthetic electron transport chain of isolated pea thylakoids. *Photosynth Res* **105**: 51-61
- Krapp AR, Rodriguez RE, Poli HO, Paladini DH, Palatnik JF, Carrillo N** (2002) The flavoenzyme ferredoxin (flavodoxin)-NADP(H) reductase modulates NADP(H) homeostasis during the soxRS response of *Escherichia coli*. *J Bacteriol* **184**: 1474-1480
- Krapp AR, Tognetti VB, Carrillo N, Acevedo A** (1997) The role of ferredoxin-NADP<sup>+</sup> reductase in the concerted cell defense against oxidative damage -- studies using *Escherichia coli* mutants and cloned plant genes. *Eur J Biochem* **249**: 556-563
- Krieger-Liszkay A, Fufezan C, Trebst A** (2008) Singlet oxygen production in photosystem II and related protection mechanism. *Photosynth Res* **98**: 551-564
- Krieger-Liszkay A, Kos PB, Hideg E** (2011) Superoxide anion radicals generated by methylviologen in photosystem I damage photosystem II. *Physiologia plantarum* **142**: 17-25
- Li J, Brader G, Kariola T, Palva ET** (2006) WRKY70 modulates the selection of signaling pathways in plant defense. *The Plant journal : for cell and molecular biology* **46**: 477-491
- Li J, Brader G, Palva ET** (2004) The WRKY70 transcription factor: a node of convergence for jasmonate-mediated and salicylate-mediated signals in plant defense. *The Plant cell* **16**: 319-331
- Lintala M, Allahverdiyeva Y, Kangasjarvi S, Lehtimaki N, Keranen M, Rintamaki E, Aro EM, Mulo P** (2009) Comparative analysis of leaf-type ferredoxin-NADP oxidoreductase isoforms in *Arabidopsis thaliana*. *Plant J* **57**: 1103-1115
- Lintala M, Allahverdiyeva Y, Kidron H, Piippo M, Battchikova N, Suorsa M, Rintamaki E, Salminen TA, Aro EM, Mulo P** (2007) Structural and functional characterization of ferredoxin-NADP<sup>+</sup>-oxidoreductase using knock-out mutants of *Arabidopsis*. *Plant J* **49**: 1041-1052
- Lintala M, Lehtimaki N, Benz JP, Jungfer A, Soll J, Aro EM, Bolter B, Mulo P** (2012) Depletion of leaf-type ferredoxin-NADP(+) oxidoreductase results in the permanent induction of photoprotective mechanisms in *Arabidopsis* chloroplasts. *Plant J* **70**: 809-817
- Lintala M, Schuck N, Thormahlen I, Jungfer A, Weber KL, Weber AP, Geigenberger P, Soll J, Bolter B, Mulo P** (2014) *Arabidopsis* tic62 trol mutant lacking thylakoid-bound ferredoxin-NADP<sup>+</sup> oxidoreductase shows distinct metabolic phenotype. *Mol Plant* **7**: 45-57
- Liochev SI, Hausladen A, Beyer WF, Jr., Fridovich I** (1994) NADPH: ferredoxin oxidoreductase acts as a paraquat diaphorase and is a member of the soxRS regulon. *Proc Natl Acad Sci U S A* **91**: 1328-1331
- Liu J, Wang P, Liu B, Feng D, Zhang J, Su J, Zhang Y, Wang JF, Wang HB** (2013) A deficiency in chloroplastic ferredoxin 2 facilitates effective photosynthetic capacity during long-term high light acclimation in *Arabidopsis thaliana*. *Plant J* **76**: 861-874
- Lu H, Rate DN, Song JT, Greenberg JT** (2003) ACD6, a novel ankyrin protein, is a regulator and an effector of salicylic acid signaling in the *Arabidopsis* defense response. *The Plant cell* **15**: 2408-2420
- Martinez-Julvez M, Medina M, Velazquez-Campoy A** (2009) Binding thermodynamics of ferredoxin:NADP<sup>+</sup> reductase: two different protein substrates and one energetics. *Biophys J* **96**: 4966-4975
- Maughan SC, Pasternak M, Cairns N, Kiddle G, Brach T, Jarvis R, Haas F, Nieuwland J, Lim B, Muller C, Salcedo-Sora E, Kruse C, Orsel M, Hell R, Miller AJ, Bray P, Foyer CH, Murray JA, Meyer AJ, Cobbett CS** (2010) Plant homologs of the *Plasmodium falciparum* chloroquine-resistance

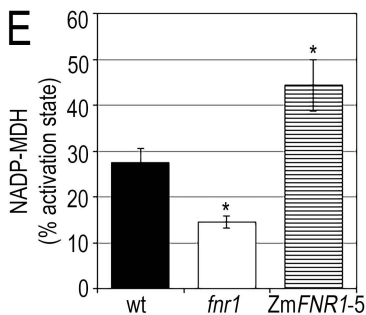
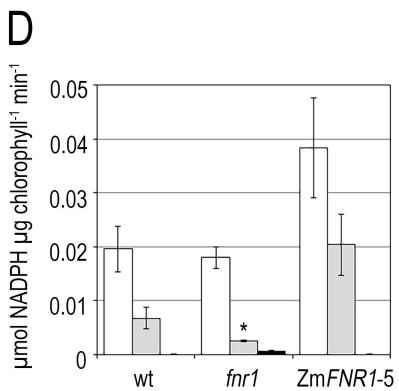
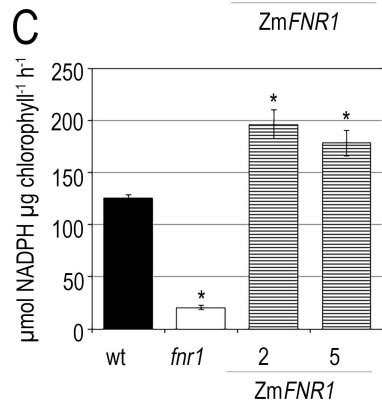
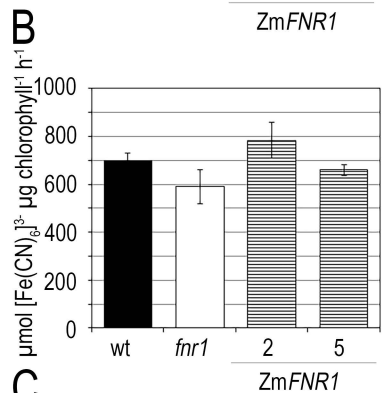
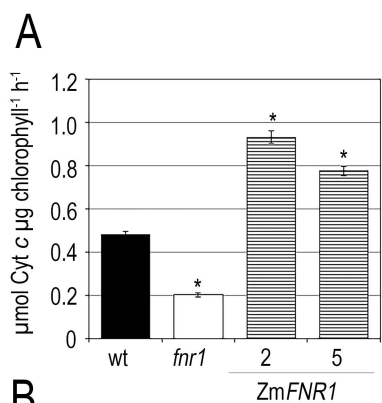
- transporter, PfcRT, are required for glutathione homeostasis and stress responses. Proceedings of the National Academy of Sciences of the United States of America **107**: 2331-2336
- Mehta RA, Fawcett TW, Porath D, Mattoo AK** (1992) Oxidative stress causes rapid membrane translocation and in vivo degradation of ribulose-1,5-bisphosphate carboxylase/oxygenase. J Biol Chem **267**: 2810-2816
- Mhamdi A, Hager J, Chaouch S, Queval G, Han Y, Tacconnat L, Saindrenan P, Gouia H, Issakidis-Bourguet E, Renou JP, Noctor G** (2010) Arabidopsis GLUTATHIONE REDUCTASE1 plays a crucial role in leaf responses to intracellular hydrogen peroxide and in ensuring appropriate gene expression through both salicylic acid and jasmonic acid signaling pathways. Plant Physiol **153**: 1144-1160
- Misra HP, Fridovich I** (1971) The Generation of Superoxide Radical during the Autoxidation of Ferredoxins. The Journal of Biological Chemistry **246**: 6886-6890
- Mittler R, Vanderauwera S, Gollery M, Van Breusegem F** (2004) Reactive oxygen gene network of plants. Trends Plant Sci **9**: 490-498
- Miyake C, Schreiber U, Hormann H, Sano S, Asada K** (1998) The FAD-Enzyme Monodehydroascorbate Radical Reductase Mediates Photoproduction of Superoxide Radicals in Spinach Thylakoid Membranes. Plant Cell Physiol **39**: 821-829
- Mou Z, Fan W, Dong X** (2003) Inducers of plant systemic acquired resistance regulate NPR1 function through redox changes. Cell **113**: 935-944
- Mowla SB, Cuyppers A, Driscoll SP, Kiddle G, Thomson J, Foyer CH, Theodoulou FL** (2006) Yeast complementation reveals a role for an Arabidopsis thaliana late embryogenesis abundant (LEA)-like protein in oxidative stress tolerance. The Plant journal : for cell and molecular biology **48**: 743-756
- Mubarakshina Borisova MM, Kozuleva MA, Rudenko NN, Naydov IA, Klenina IB, Ivanov BN** (2012) Photosynthetic electron flow to oxygen and diffusion of hydrogen peroxide through the chloroplast envelope via aquaporins. Biochim Biophys Acta **1817**: 1314-1321
- Oelze ML, Kandlbinder A, Dietz KJ** (2008) Redox regulation and overreduction control in the photosynthesizing cell: complexity in redox regulatory networks. Biochim Biophys Acta **1780**: 1261-1272
- Okutani S, Hanke GT, Satomi Y, Takao T, Kurisu G, Suzuki A, Hase T** (2005) Three maize leaf ferredoxin:NADPH oxidoreductases vary in subchloroplast location, expression, and interaction with ferredoxin. Plant physiology **139**: 1451-1459
- Palatnik JF, Tognetti VB, Poli HO, Rodriguez RE, Blanco N, Gattuso M, Hajirezaei MR, Sonnewald U, Valle EM, Carrillo N** (2003) Transgenic tobacco plants expressing antisense ferredoxin-NADP(H) reductase transcripts display increased susceptibility to photo-oxidative damage. Plant J **35**: 332-341
- Palatnik JF, Valle EM, Carrillo N** (1997) Oxidative stress causes ferredoxin-NADP+ reductase solubilization from the thylakoid membranes in methyl viologen-treated plants. Plant Physiol **115**: 1721-1727
- Pulido P, Spinola MC, Kirchsteiger K, Guinea M, Pascual MB, Sahrawy M, Sandalio LM, Dietz KJ, Gonzalez M, Cejudo FJ** (2010) Functional analysis of the pathways for 2-Cys peroxiredoxin reduction in Arabidopsis thaliana chloroplasts. J Exp Bot **61**: 4043-4054
- Queval G, Jaillard D, Zechmann B, Noctor G** (2011) Increased intracellular H<sub>2</sub>O<sub>2</sub> availability preferentially drives glutathione accumulation in vacuoles and chloroplasts. Plant Cell Environ **34**: 21-32
- Rao MV, Paliyath G, Ormrod DP, Murr DP, Watkins CB** (1997) Influence of salicylic acid on H<sub>2</sub>O<sub>2</sub> production, oxidative stress, and H<sub>2</sub>O<sub>2</sub>-metabolizing enzymes. Salicylic acid-mediated oxidative damage requires H<sub>2</sub>O<sub>2</sub>. Plant Physiol **115**: 137-149
- Rodriguez RE, Lodeyro A, Poli HO, Zurbriggen M, Peisker M, Palatnik JF, Tognetti VB, Tschiersch H, Hajirezaei MR, Valle EM, Carrillo N** (2007) Transgenic tobacco plants overexpressing

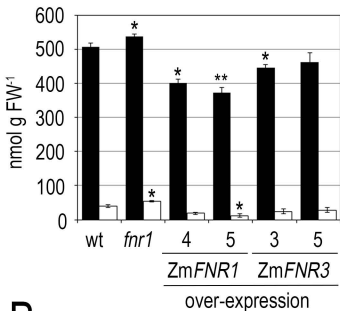
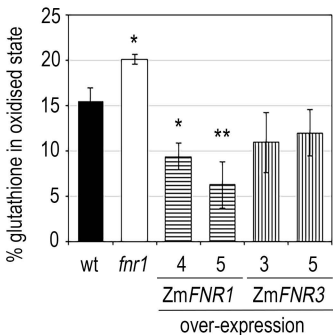


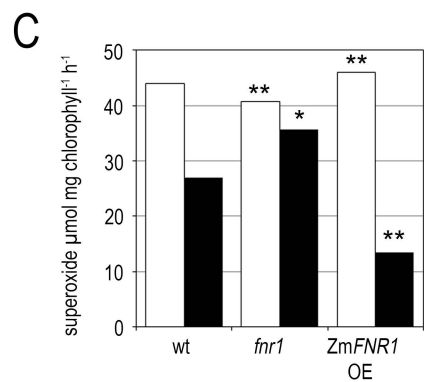
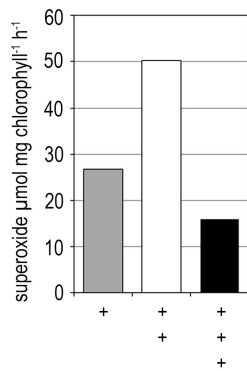
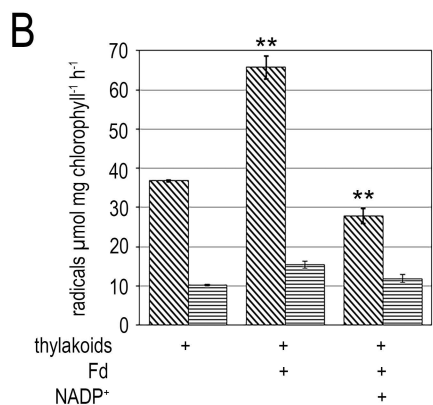
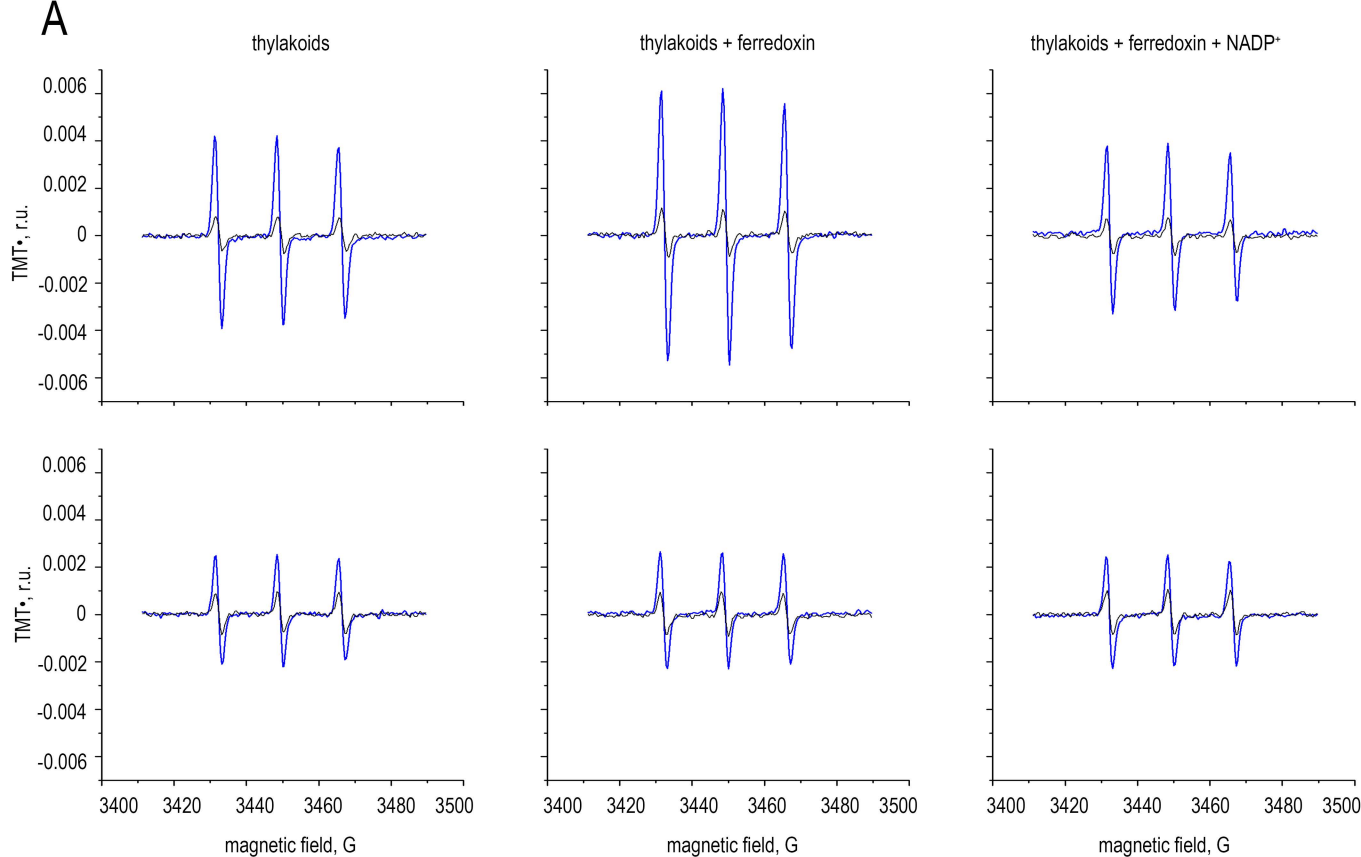
- chloroplastic ferredoxin-NADP(H) reductase display normal rates of photosynthesis and increased tolerance to oxidative stress. *Plant Physiol* **143**: 639-649
- Salleh FM, Evans K, Goodall B, Machin H, Mowla SB, Mur LA, Runions J, Theodoulou FL, Foyer CH, Rogers HJ** (2012) A novel function for a redox-related LEA protein (SAG21/AtLEA5) in root development and biotic stress responses. *Plant, cell & environment* **35**: 418-429
- Scheibe R** (2004) Malate valves to balance cellular energy supply. *Physiologia plantarum* **120**: 21-26
- Scheibe R, Backhausen JE, Emmerlich V, Holtgreffe S** (2005) Strategies to maintain redox homeostasis during photosynthesis under changing conditions. *Journal of experimental botany* **56**: 1481-1489
- Scheibe R, Dietz KJ** (2012) Reduction-oxidation network for flexible adjustment of cellular metabolism in photoautotrophic cells. *Plant Cell Environ* **35**: 202-216
- Scheibe R, Stitt M** (1988) Comparison of NADP-malate dehydrogenase activation, QA reduction and O<sub>2</sub> evolution in spinach leaves. *Plant Physiology and Biochemistry* **26**: 473-481
- Schurmann P, Buchanan BB** (2008) The ferredoxin/thioredoxin system of oxygenic photosynthesis. *Antioxid Redox Signal* **10**: 1235-1274
- Shim JS, Jung C, Lee S, Min K, Lee YW, Choi Y, Lee JS, Song JT, Kim JK, Choi YD** (2013) AtMYB44 regulates WRKY70 expression and modulates antagonistic interaction between salicylic acid and jasmonic acid signaling. *The Plant journal : for cell and molecular biology* **73**: 483-495
- Snyrychova I, Pospisil P, Naus J** (2006) Reaction pathways involved in the production of hydroxyl radicals in thylakoid membrane: EPR spin-trapping study. *Photochem Photobiol Sci* **5**: 472-476
- Tateda C, Zhang Z, Greenberg JT** (2015) Linking pattern recognition and salicylic acid responses in Arabidopsis through ACCELERATED CELL DEATH6 and receptors. *Plant signaling & behavior* **10**: e1010912
- Telfer A, Bishop SM, Phillips D, Barber J** (1994) Isolated photosynthetic reaction center of photosystem II as a sensitizer for the formation of singlet oxygen. Detection and quantum yield determination using a chemical trapping technique. *J Biol Chem* **269**: 13244-13253
- Tognetti VB, Palatnik JF, Fillat MF, Melzer M, Hajirezaei MR, Valle EM, Carrillo N** (2006) Functional replacement of ferredoxin by a cyanobacterial flavodoxin in tobacco confers broad-range stress tolerance. *Plant Cell* **18**: 2035-2050
- Twachtmann M, Altmann B, Muraki N, Voss I, Okutani S, Kurisu G, Hase T, Hanke GT** (2012) N-terminal structure of maize ferredoxin:NADP<sup>+</sup> reductase determines recruitment into different thylakoid membrane complexes. *Plant Cell* **24**: 2979-2991
- Ulker B, Shahid Mukhtar M, Somssich IE** (2007) The WRKY70 transcription factor of Arabidopsis influences both the plant senescence and defense signaling pathways. *Planta* **226**: 125-137
- Van Eck L, Davidson RM, Wu S, Zhao BY, Botha AM, Leach JE, Lapitan NL** (2014) The transcriptional network of WRKY53 in cereals links oxidative responses to biotic and abiotic stress inputs. *Functional & integrative genomics* **14**: 351-362
- Vojta L, Caric D, Cesar V, Antunovic Dunic J, Lepedus H, Kveder M, Fulgosi H** (2015) TROL-FNR interaction reveals alternative pathways of electron partitioning in photosynthesis. *Scientific reports* **5**: 10085
- Wagner D, Przybyla D, Op den Camp R, Kim C, Landgraf F, Lee KP, Wursch M, Laloï C, Nater M, Hideg E, Apel K** (2004) The genetic basis of singlet oxygen-induced stress responses of Arabidopsis thaliana. *Science* **306**: 1183-1185
- Yamauchi Y, Hasegawa A, Mizutani M, Sugimoto Y** (2012) Chloroplastic NADPH-dependent alkenal/one oxidoreductase contributes to the detoxification of reactive carbonyls produced under oxidative stress. *FEBS Lett* **586**: 1208-1213
- Yang C, Hu H, Ren H, Kong Y, Lin H, Guo J, Wang L, He Y, Ding X, Grabsztunowicz M, Mulo P, Chen T, Liu Y, Wu Z, Wu Y, Mao C, Wu P, Mo X** (2016) LIGHT-INDUCED RICE1 Regulates Light-Dependent Attachment of LEAF-TYPE FERREDOXIN-NADP<sup>+</sup> OXIDOREDUCTASE to the Thylakoid Membrane in Rice and Arabidopsis. *The Plant cell* **28**: 712-728

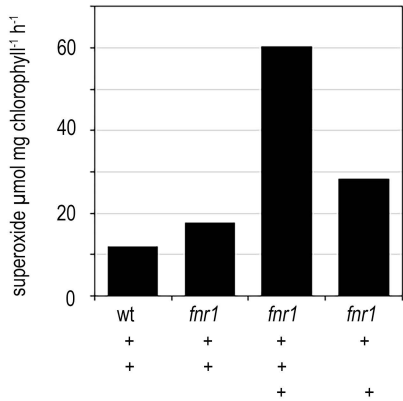
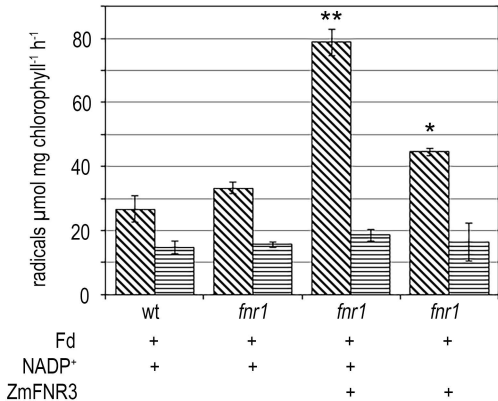
- Zhang H, Whitelegge JP, Cramer WA** (2001) Ferredoxin:NADP<sup>+</sup> oxidoreductase is a subunit of the chloroplast cytochrome b6f complex. *J Biol Chem* **276**: 38159-38165
- Zhang Z, Feechan A, Pedersen C, Newman MA, Qiu JL, Olesen KL, Thordal-Christensen H** (2007) A SNARE-protein has opposing functions in penetration resistance and defence signalling pathways. *The Plant journal : for cell and molecular biology* **49**: 302-312
- Zhang Z, Lenk A, Andersson MX, Gjetting T, Pedersen C, Nielsen ME, Newman MA, Hou BH, Somerville SC, Thordal-Christensen H** (2008) A lesion-mimic syntaxin double mutant in *Arabidopsis* reveals novel complexity of pathogen defense signaling. *Molecular plant* **1**: 510-527

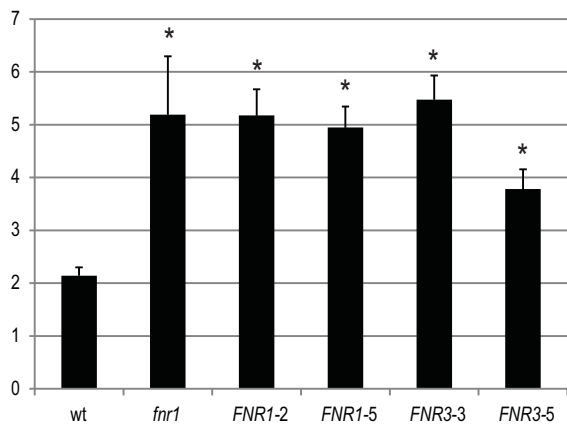
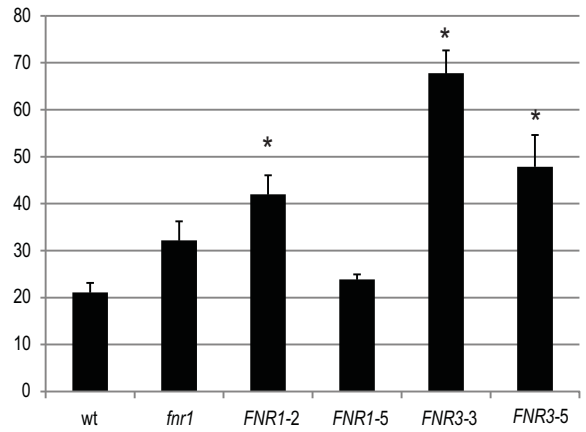
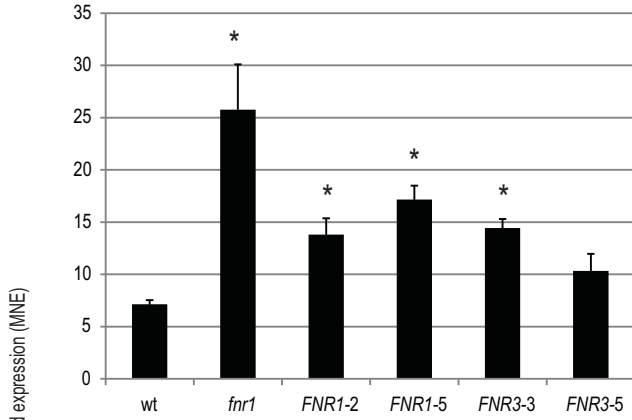
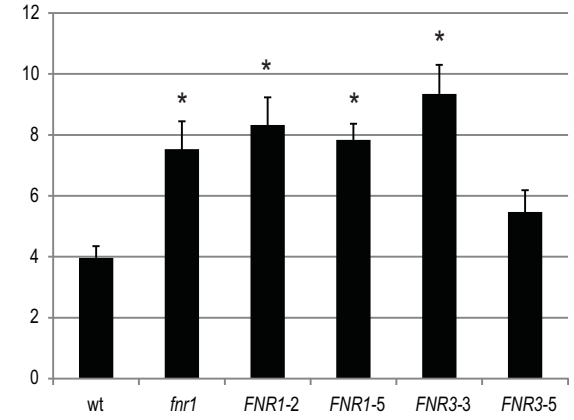
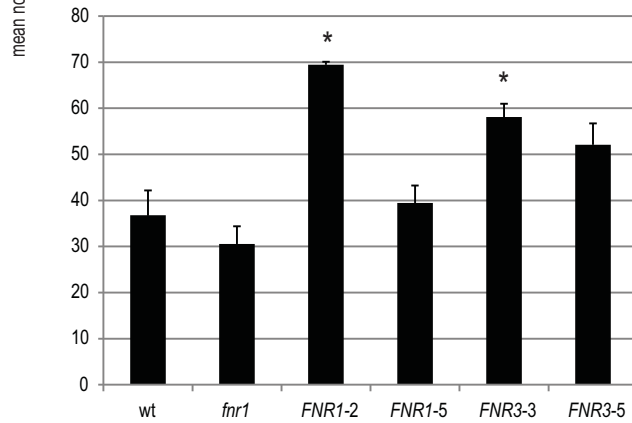
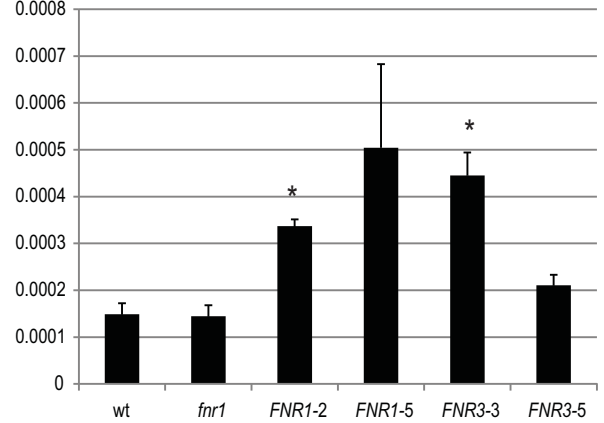
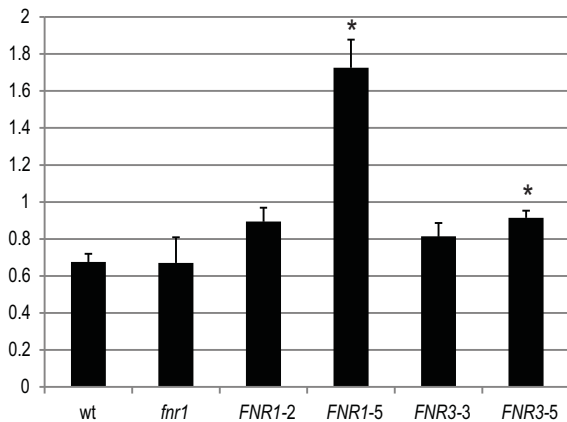




**A****B**





**WRKY53****WRKY70****LEA5/SAG21****SYPI22****ACD6****Dirigent 5****At2g21640 (oxidative stress marker)****NADP-MDH**